A Semi-Synthetic Ion Channel Platform for Detection of Phosphatase and Protease Activity

Michael X. Macrae,[†,§] Steven Blake,[†,§] Xiayun Jiang,[‡] Ricardo Capone,[‡] Daniel J. Estes,[‡] Michael Mayer,[‡,*] and Jerry Yang[†,*]

[†]Department of Chemistry and Biochemistry, University of California, San Diego, 9500 Gilman Drive, MC 0358, La Jolla, California 92093-0358 and [‡]Department of Biomedical Engineering and Department of Chemical Engineering, University of Michigan, 1101 Beal Avenue, Ann Arbor, Michigan 48109-2110. [§]These authors contributed equally.

ABSTRACT Sensitive methods to probe the activity of enzymes are important for clinical assays and for elucidating the role of these proteins in complex biochemical networks. This paper describes a semi-synthetic ion channel platform for detecting the activity of two different classes of enzymes with high sensitivity. In the first case, this method uses single ion channel conductance measurements to follow the enzyme-catalyzed hydrolysis of a phosphate group attached to the C-terminus of gramicidin A (gA, an ion channel-forming peptide) in the presence of alkaline phosphatase (AP). Enzymatic hydrolysis of this phosphate group removes negative charges from the entrance of the gA pore, resulting in a product with measurably reduced single ion channel conductance compared to the original gA—phosphate substrate. This technique employs a standard, commercial bilayer setup and takes advantage of the catalytic turnover of enzymes and the amplification characteristics of ion flux through individual gA pores to detect picomolar concentrations of active AP in solution. Furthermore, this technique makes it possible to study the kinetics of an enzyme and provides an estimate for the observed rate constant (k_{cat}) and the Michaelis constant (K_M) by following the conversion of the gA—phosphate substrate to product over time in the presence of different concentrations of AP. In the second case, modification of gA with a substrate for proteolytic cleavage by anthrax lethal factor (LF) afforded a sensitive method for detection of LF activity, illustrating the utility of ion channel-based sensing for detection of a potential biowarfare agent. This ion channel-based platform represents a powerful, novel approach to monitor the activity of femtomoles to picomoles of two different classes of enzymes in solution. Furthermore, this platform has the potential for realizing miniaturized, cost-effective bioanalytical assays that complement currently established assays.

KEYWORDS: gramicidin A · alkaline phosphatase (AP) · planar lipid bilayers · ion channels · biosensors · enzyme activity · anthrax lethal factor (LF) · biowarfare agent

This paper presents a single channel recording platform for monitoring the activity of enzymes through their reaction with substrates attached to the ion channel-forming peptide gramicidin A (gA). This platform exploits the catalytic activity of an enzyme in combination with the amplification characteristics of ion conductance through individual gA pores to detect picomolar to nanomolar concentrations of active proteins in solution.

The activity of enzymes can be indicative of normal or abnormal cellular function and is often used to diagnose diseases or to detect infections.[1−3] Here, we investigated alkaline phosphatase (AP) and anthrax lethal factor (LF) as two model enzymes to develop a gA-based, planar lipid bilayer platform (Figure 1) as a sensitive analytical strategy for *in situ* detection of enzyme activity. Assessing AP activity in blood is a routine part of health examinations because abnormal levels can be early indicators of cancer[4,5] or liver damage.[6,7] Detecting LF at low concentrations is relevant in the context of bioterrorism because *Bacillus anthracis* is classified as a biowarfare agent[8−12] and because sensitive methods for detection of LF are important for early determination of infection by *B. anthracis*.[13] Although colorimetric,[14−17] chromatographic,[18−20] electrochemical,[21−23] and ELISA-based[24,25] methods have been developed to quantify the activity of clinically relevant enzymes, new diagnostic platforms are still needed to improve the robustness, sensitivity, selectivity, portability, speed, and cost-effectiveness of bioanalytical assays.

To date, only three examples of ion channel recordings for detecting enzyme activity have been reported. In all three cases, α-hemolysin pores were used as the sensing element.[26] In the first case, Ghadiri's group recently reported the use of ion channel conductance to detect single-nucleotide primer extensions catalyzed by DNA polymerase.[27] In the second case, Bayley's group detected the activity of an exonuclease in an effort to explore the potential of α-hemolysin pores for DNA sequencing.[28] In the most recent case, Zhao *et al.* reported the detection of trypsin activity by monitoring the translocation of cleavage products through an α-hemolysin pore.[29]

*Address correspondence to jerryyang@ucsd.edu, mimayer@umich.edu.

Received for review September 15, 2009 and accepted October 18, 2009.

Published online October 27, 2009. 10.1021/nn901231h CCC: $40.75

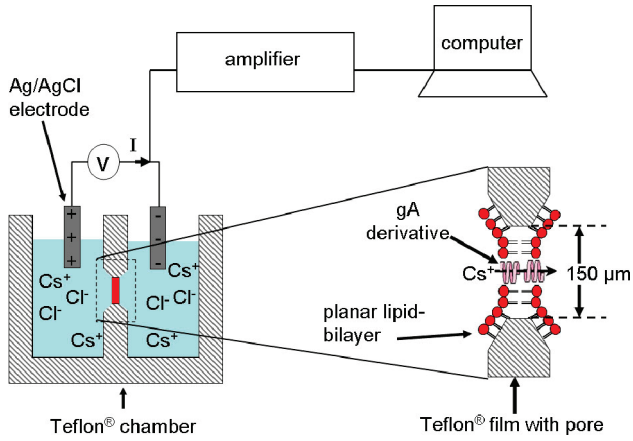

Figure 1. Illustration of a planar lipid bilayer setup for recording single ion channel currents through derivatives of gramicidin A. The Teflon chamber consists of two compartments filled with a recording electrolyte containing CsCl as a source of monovalent cations. The two aqueous compartments are separated by a Teflon film with a small aperture that supports a planar lipid bilayer. Each compartment contains one Ag/AgCl electrode that is submerged in the recording electrolyte. When a voltage is applied by a patch clamp amplifier, cesium cations pass through pores formed by two molecules of a gA derivative (embedded in the bilayer) and create a measurable current. A computer is used to store and analyze the recorded single channel currents.

The research presented here explores an alternative and novel ion channel-based strategy for the detection of enzymatic activity by monitoring changes in single channel conductance through a gramicidin pore upon reaction of enzymes with substrates attached covalently to the C-terminus of gA. This platform offers at least four complementary advantages for detection of enzyme activity compared to methods that are not based on ion channels. These advantages include: (1) the method utilizes the amplification characteristics of modulated ion flux through a single ion channel to achieve high sensitivity (by modifying individual ion pores and consequently affecting the flux of thousands of ions);[30−37] (2) the method is orthogonal to colorimetric assays and can, therefore, be advantageous for solutions that are colored, contain fluorescent molecules, or quenchers of fluorescence (*e.g.*, blood);[30,38] (3) the method requires only extremely small quantities (subpicomole amounts) of the ion channel probe (minimizing cost); and (4) the nanoscale size of ion channels makes it possible to develop enzyme activity assays within miniaturized, cost-effective, and potentially portable, low power devices.[39−42] In contrast to α-hemolysin, which forms permanent pores in bilayers,[43] gA reversibly partitions into and out of lipid bilayers (with a strong preference for the bilayer[44]) facilitating stepwise transmembrane flux of monovalent cations upon dynamic dimerization and dissociation.[45,46] These stepwise fluctuations in recorded single channel current, which are a consequence of dynamic opening and closing of gA pores, make it possible to determine the single channel conductance of gA pores with high accuracy; measurement of the single channel conductance through gA pores is hence independent of possible artifacts that may affect the ion permeability through the entire area of the bilayer. Permanent pores, such as α-hemolysin, do not provide this advantage because of the absence of complete opening and closing steps. Additionally, since gA reversibly partitions between the membrane and the bulk electrolyte solution, sensors based on a gA platform[47−55] can participate in homogeneous processes occurring in the bulk solution, whereas permanently incorporated pores are limited to heterogeneous processes on a membrane surface.[56] Furthermore, gA is particularly well-suited for the development of an ion channel-based assay to detect enzyme activity because it is available in gram-scale quantities and conducive to synthetic derivatization while preserving its ion channel function;[52,57−63] it can be tailored for the detection of specific chemically or biochemically reactive analytes,[30,38,50,52,54,55,60−65] and it is simple to use due to its spontaneous self-incorporation into bilayers and its well-defined, discrete ion conductance values.

We previously reported that single ion channel recordings can be used to detect, *in situ*, the reactivity of molecules in solution if they chemically modify the ionic charge on functional groups near the opening of a gA pore (we call this mode of detection charge-based sensing).[30,38,52] According to the Gouy−Chapman theory,[66] a charged group presented at a bilayer surface can cause a significant change in the local concentration of ions[67] (especially at low ionic strength[30]).[68] This change in local ion concentration can, in turn, affect the conductance of ion channels that are embedded in a bilayer. The resulting modulation in single channel conductance makes it possible to detect a reaction that alters the charge on substrates attached to the entrance of an ion pore.[30,38,52]

Here, we explored whether charge-based sensing could be used to detect the enzyme activity of AP through its capability to catalyze the hydrolysis of negatively charged phosphate groups from substrates attached to the C-terminus of gA. We demonstrate that enzymatic hydrolysis of a phosphate group from gA, and the concomitant removal of negative charges from the entrance of the gA pore, resulted in a significant change in single channel conductance. This research represents the first example of using gramicidin pores for the direct detection of enzyme activity by monitoring changes in single ion channel conductance. Furthermore, we demonstrate that single ion channel conductance measurements can be used to monitor the kinetics of AP, making it possible to provide an estimate of the observed rate constant (k_{cat}) and the Michaelis constant (K_M) of the enzyme-catalyzed reaction. Finally, in order to illustrate that this ion channel-based sensing platform could be applied to a second class of enzymes, we show that a gA derivative with a covalently attached substrate for anthrax lethal factor

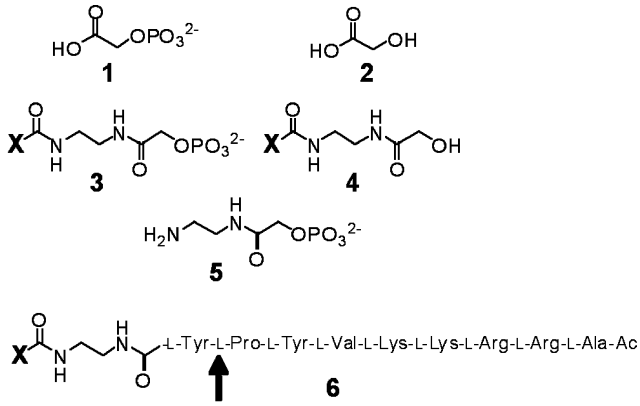

Figure 2. Structures of glycolic acid-*O*-phosphate 1, glycolic acid 2, a derivative of gramicidamine[30,52] carrying a glycolic acid-*O*-phosphate (3, gA−phosphate), a derivative of gramicidamine[30,52] carrying glycolic acid 4, an O-phosphorylated derivative of ethylenediamine-*N*-glycolate 5, and a derivative of gA carrying a substrate for LF (gA−LF substrate 6). The arrow indicates the site of cleavage of 6 by LF.

(LF) made it possible to detect the protease activity of this enzyme *in situ*, in real time, and at concentrations of LF as low as 10 nM.

RESULTS AND DISCUSSION

A gA-Based Sensor for Detection of Alkaline Phosphatase. In order to develop a substrate for AP that we could readily attach to the opening of a gA pore, we investigated the reactivity of AP with glycolic acid-*O*-phosphate (Figure 2, molecule **1**). We chose **1** as a substrate since, after attaching it to the C-terminus of gA (as shown in molecule **3**, Figure 2), it presents a negatively charged phosphate group in close proximity to the opening of the pore (a property that is important for charge-based sensing[30]). Since AP is a promiscuous enzyme that reacts with a variety of organic phosphates,[69] we hypothesized that **1** would act as a substrate for AP. We confirmed by ^{31}P NMR spectroscopy that a 14 mM solution of **1** was completely hydrolyzed to glycolic acid **2** by 2 μM AP (from bovine intestinal mucosa, EC 3.1.3.1) within 50 min. In a control experiment, we did not observe any hydrolysis of **1** over the course of 24 h when AP was not present in these NMR experiments.

We also measured the single channel conductance of gA−phosphate (**3**) and its hydrolysis product (**4**) (see Figure S1 in the Supporting Information) by incorporating them into a planar lipid bilayer setup (Figure 1). Figure 3 shows representative current *versus* time traces of **3** and **4** under an applied potential of 75 mV in buffered recording electrolyte. These current traces show that **3** had a significantly larger conductance (by a factor of ~2.2) than **4** in this recording electrolyte. We attribute this difference to an electrostatically induced local increase in the concentration of cesium cations near the negatively charged phosphate group presented at opening of the ion pore in **3**.[30] Analysis of the current *versus* voltage ($I-V$) curves of **3** and **4** revealed single channel conductance values (γ) of 13.0 ± 0.4 pS for **3** and 5.8 ± 0.2 pS for **4** in this recording electrolyte (see Figure S1 in the Supporting Information).[70] These results suggest that single ion channel conductance measurements can be used to distinguish between gA derivatives **3** and **4**; these measurements, therefore, make it possible to detect the dephosphorylating activity of AP.

In order to test if the enzyme activity of AP could be detected *in situ* by monitoring single ion channel currents in solutions that contained AP, we added **3** to a final concentration of 15 pM to both compartments of a planar lipid bilayer setup containing the recording electrolyte (Figure 1). We subsequently added AP to a final concentration of 600 nM and monitored the enzymatic conversion of **3** to **4** over time (Figure 4). Comparing the percentage of single ion channel events from **4** to the percentage of single ion channel events from **3** throughout the course of the reaction then made it possible to quantify the time-dependent conversion of **3** to **4**. We defined the fraction of ion channel events from **4** (f_4) as the number of events originating from **4** ($\gamma \approx$ 6 pS) divided by the total number of events (from **3** and **4**) observed during a 5 or 10 min interval of recording. Similarly, we defined the fraction of ion channel events from **3** (f_3) as the number of events originating from **3** ($\gamma \approx$ 13 pS) divided by the total number of events observed during a 5 or 10 min interval of recording.

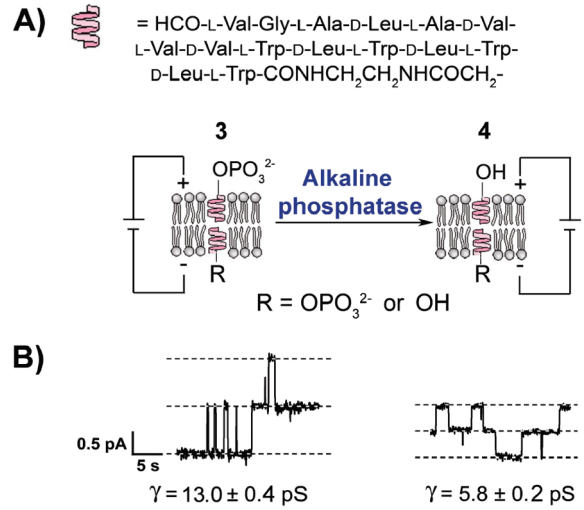

Figure 3. Cartoon illustrating the detection of alkaline phosphatase (AP) activity using an ion channel platform. (A) Conversion of a negatively charged phosphate group on gA derivative 3 to a neutral alcohol in the presence of AP. (B) Representative single ion channel recordings of 3 and 4, as well as the respective single channel conductance values, γ. These original current *versus* time traces were recorded using as electrolyte a buffered solution containing 50 mM CsCl, 1 mM $MgCl_2$, and 0.5 mM K_2CO_3 at pH 9.8 (recording buffer). The applied potential was +75 mV.

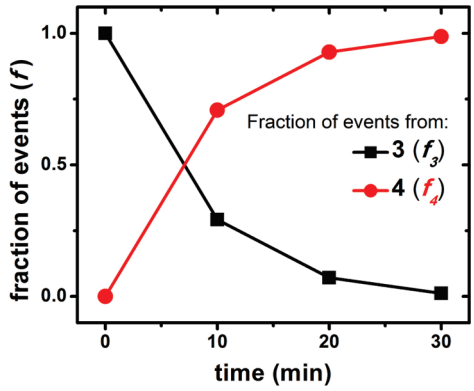

Figure 4. Time-dependent enzymatic hydrolysis of the phosphate group on 3 to 4 in the presence of 600 nM AP as determined using single ion channel conductance measurements. We estimated the fraction of total ion channel events corresponding to 3 (f_3) or 4 (f_4) over time by counting the number of big ($\gamma \approx 13$ pS) and small ($\gamma \approx 6$ pS) events within 5 min time intervals (the total number of single ion channel events counted was greater than 50 for each time interval); these intervals were separated by 10 min.

Figure 4 shows that, while the enzymatic reaction progressed in the bilayer chamber, the fraction of single ion channel events from gA-phosphate **3**, f_3, decreased, whereas the fraction of events from the hydrolysis product **4**, f_4, increased. Figure 4 also illustrates that, after 30 min, almost all recorded ion channel events originated from the hydrolysis product **4**. In the absence of AP, we did not observe any hydrolysis of **3** to **4** in these ion channel experiments over the course of 1 h.

In order to demonstrate the sensitivity of the assay, we show in Figure 5A that these *in situ* measurements of ion channel events made it possible to monitor the hydrolysis of **3** to **4** catalyzed by AP at enzyme concentrations as low as 600 pM (Figure S2 in the Supporting Information shows a representative example for the time-dependent change in the frequency of ion channel events from **3** and **4** in the presence of AP). In order to demonstrate the reproducibility of these *in situ* experiments, Figure 5A also shows a comparison of two independent experiments that monitored the hydrolysis of **3** to **4** in the presence of 60 nM AP. The calculated initial slopes of the exponential fits to the data from these two experiments (red and gray curve in Figure 5A) were 0.031 ± 0.004 min^{-1} ($R^2 = 0.91$, $N = 8$) and 0.032 ± 0.003 min^{-1} ($R^2 = 0.94$, $N = 8$), respectively. The reproducibility of this technique was, therefore, very good (variation $\leq$4%).

Limit of Detection of AP Activity Using the Gramicidin-Based Assay. To explore whether the detection limit of this ion channel assay could be extended to concentrations of AP below 600 pM, reaction times exceeding 7 h would be required to achieve detectable hydrolysis of **3** to **4**. Bilayer experiments are, however, typically restricted to a few hours due to the limited stability of the bilayer membrane.[49,71] In order to afford extended reaction times, we incubated samples of **3** with solutions of AP at concentrations ranging from 6 pM to 6 nM in reaction vials

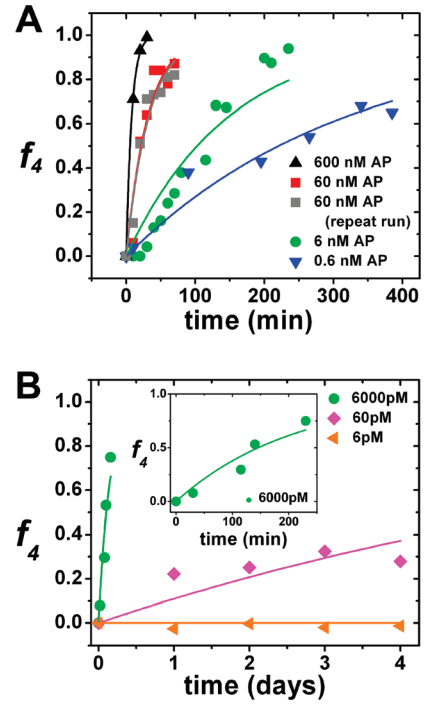

Figure 5. Monitoring the fraction of ion channel events from the enzymatic product 4, f_4, over time at various concentrations of AP. (A) *In situ* detection of the hydrolysis of 15 pM 3 in the presence of 600 pM to 600 nM AP. (B) *Ex situ* detection of the hydrolysis of 3 to 4 over 4 days. For these *ex situ* experiments, solutions containing 150 pM gA derivative 3 were incubated with AP concentrations of 6 pM (orange), 60 pM (magenta), or 6 nM (green) in reaction vials (outside of the bilayer chamber) at 23 °C. We analyzed the progression of these reactions in daily intervals by introducing aliquots of the reaction mixture to the planar lipid bilayer setup. The inset in (B) shows the data for the conversion of 3 to 4 catalyzed by 6 nM AP (solid green circles) with expanded time axis in order to facilitate a comparison between the *ex situ* and *in situ* experiments. Data were fit to a first-order exponential function of the form $f_4 = (1 - e^{-k_{cat} \times [AP]_T \times t})$, where t is the reaction time, and k_{cat} (the fitting parameter) is the observed pseudo-first-order rate constant for a given total concentration of AP, $[AP]_T$.

(*i.e.*, outside of the bilayer setup) for 4 days and we analyzed samples periodically for single ion channel events. Figure 5B shows that this *ex situ* incubation strategy made it possible to detect 60 pM concentrations of AP, corresponding to femtomoles of enzyme in the reaction vials. In addition, the inset in Figure 5B shows that the progression of hydrolysis of **3** catalyzed by 6 nM AP using this *ex situ* protocol was comparable (within a factor of ~1.2) with *in situ* measurement of the hydrolysis of **3** to **4** using the same concentration of enzyme. The small discrepancy of 20% in measured rate between the *ex situ* and *in situ* protocols may partly be attributable to differential adsorption of **3** and **4** to the reaction vials during *ex situ* experiments. This result suggests that the presence of a lipid membrane during the enzymatic reaction did not have a strong effect on the rate of hydrolysis, despite the amphiphilic character of the enzyme substrate **3**.

Kinetic Analysis of the Enzymatic Activity of AP. Figure 5 establishes that ion channel-based sensing can be used

to detect femtomoles to picomoles of active AP in solution. To assess if this technique could also reveal information about the kinetics of this AP-catalyzed reaction, we obtained the initial reaction rates of hydrolysis (initial velocity, V_0) of **3** to **4** as a function of enzyme concentration from the *in situ* data in Figure 5A. For this analysis, we made the following three assumptions: (1) the hydrolysis of **3** to **4** takes place in the absence of significant competing processes (such as the time-dependent decomposition of the enzyme); (2) the degree of partitioning of **3** and **4** into the bilayer is the same under the applied recording conditions; and (3) the frequency of ion channel events from molecule **3** depends on the concentration of **3** in the same way as the frequency of events from **4** depends on the concentration of **4**.

Starting from the simplest form of the standard rate equation, the velocity, V, of this enzymatic reaction can be described as

$$V = -\frac{d[\mathbf{3}]}{dt} = k_{cat}[AP]_T[\mathbf{3}] \quad (1)$$

where k_{cat} represents the observed rate constant and $[AP]_T$ represents the total enzyme concentration.[72] Equation 1 assumes that the concentration of free AP, [AP], is close to $[AP]_T$. Since the lowest concentration of AP used to generate the data in Figure 5A was 40 times higher than the initial concentration of **3** ($[\mathbf{3}]_0$), this assumption is adequate for all data shown in Figure 5A. Rearrangement of eq 1 and integration gives

$$\frac{[\mathbf{3}]}{[\mathbf{3}]_0} = e^{-k_{cat}[AP]_T t} \quad (2)$$

In order to relate eq 2 to the fraction of ion channel events from **4**, f_4, we substitute [**3**] in eq 2 with $[\mathbf{3}] = [\mathbf{3}]_0 - [\mathbf{4}]$ and rearrange

$$\frac{[\mathbf{4}]}{[\mathbf{3}]_0} = (1 - e^{-k_{cat}[AP]_T t}) \quad (3)$$

By making the approximation that the frequency of events from **4** is linearly dependent on the concentration of **4** (see the Supporting Information for a discussion on the relationship between f_4 and the concentration of **4**), and based on the previously stated assumption that the frequency of ion channel events from molecule **3** depends on the concentration of **3** in the same way as the frequency of events from **4** depends on the concentration of **4**, we obtain the fraction of ion channel events from **4**, f_4:

$$f_4 = \frac{[\mathbf{4}]}{[\mathbf{3}] + [\mathbf{4}]} = \frac{[\mathbf{4}]}{[\mathbf{3}]_0} \quad (4)$$

Combining eqs 3 and 4 gives the functional dependence of f_4 on k_{cat}, $[AP]_T$, and time:

$$f_4 = \frac{[\mathbf{4}]}{[\mathbf{3}]_0} = (1 - e^{-k_{cat}[AP]_T t}) \quad (5)$$

Fitting the data in Figure 5A to eq 5 returned the value of k_{cat} as the only fitting parameter for each concentration of enzyme ($[AP]_T$). To obtain the initial velocities of these AP-catalyzed reactions, we differentiated eq 5:

$$\frac{df_4}{dt} = \frac{d[\mathbf{4}]}{[\mathbf{3}]_0 dt} = \frac{d(1 - e^{-k_{cat}[AP]_T t})}{dt} = k_{cat}[AP]_T e^{-k_{cat}[AP]_T t} \quad (6)$$

Since the velocity of the AP-catalyzed reaction is

$$V = \frac{d[\mathbf{4}]}{dt} \quad (7)$$

we obtain eq 8 by combining eqs 6 and 7:

$$V = \frac{d[\mathbf{4}]}{dt} = \frac{[\mathbf{3}]_0 df_4}{dt} = k_{cat}[AP]_T[\mathbf{3}]_0 e^{-k_{cat}[AP]_T t} \quad (8)$$

The initial velocity (V_0) at $t = 0$ s for a given total concentration of enzyme, $[AP]_T$, can, therefore, be written as

$$V_0 = k_{cat}[AP]_T[\mathbf{3}]_0 \quad (9)$$

Equation 9 shows that values for V_0 can be obtained from $[\mathbf{3}]_0$ multiplied by $[AP]_T$ multiplied by the values of k_{cat} that we obtained from the best curve fit of the data in Figure 5A with eq 5. Figure 6 shows the resulting graphical representation of V_0 *versus* $[AP]_T$ from *in situ* experiments.

In the standard analysis of enzyme kinetics, the Michaelis−Menten (MM) equation describes the relationship between the initial velocity as a function of free substrate and total enzyme concentration. The MM equation is defined as $V_0 = V_{max}[\mathbf{3}]/(K_M + [\mathbf{3}])$, where $V_{max} = k_{cat}[AP]_T$ and K_M represents the Michaelis constant.[72−74] For conditions in which [**3**] cannot be assumed to be close to $[\mathbf{3}]_T$ (such as for the experimental conditions used to generate the data shown in Figure 5A, where the concentration of enzyme was in excess), standard MM analysis is not adequate. Instead, Morrison derived a modified MM equation that accounts for these conditions and that relates velocity, V, of the en-

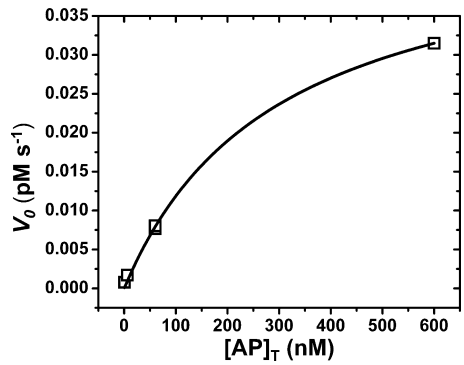

Figure 6. Kinetic analysis of the initial rates (V_0) for the hydrolysis of 3 to 4 *versus* the total concentration of AP. The solid curve represents a best curve fit of the data with eq 11. This fit returned $k_{cat} = (3.1 \pm 0.2) \times 10^{-3}$ s^{-1} and $K_M = (3.0 \pm 0.4) \times 10^{-7}$ M as fitting parameters ($R^2 = 0.99$, $N = 5$).

zyme reaction to the total concentrations of substrate ($[\mathbf{3}]_T$) and enzyme ($[AP]_T$):[75]

$$V = V_{max}\frac{a - \sqrt{a^2 - 4[AP]_T[\mathbf{3}]_T}}{2[AP]_T} \quad (10)$$

where $a = ([AP]_T + [\mathbf{3}]_T + K_M)$. Under initial rate conditions, $[\mathbf{3}]_T$ is equal to $[\mathbf{3}]_0$ and V is equal to V_0. The Morrison equation can, therefore, be written as (with $V_{max} = k_{cat}[AP]_T$):

$$V = k_{cat}\frac{b - \sqrt{b^2 - 4[AP]_T[\mathbf{3}]_0}}{2} \quad (11)$$

where $b = ([AP]_T + [\mathbf{3}]_T + K_M)$.

In order to obtain estimates for k_{cat} and K_M, we used this eq 11 to fit the data in Figure 6, where k_{cat} and K_M are fitting parameters. The saturation behavior shown in Figure 6 is a consequence of the depletion of free substrate at increasing AP concentrations. The excellent fit of the data in Figure 6 ($R^2 = 0.99$, $N = 5$) with eq 11 demonstrates that the Morrison equation (eq 10) appropriately models the kinetics of this enzyme under these conditions.[75] From this best fit analysis of the *in situ* data in Figure 6 with eq 11, we obtained a value of $k_{cat} = (3.1 \pm 0.2) \times 10^{-3}$ s^{-1} and a value of $K_M = (3.0 \pm 0.4) \times 10^{-7}$ M. An additional parameter obtained from MM kinetics is the catalytic efficiency (k_{cat}/K_M), which provides a measure for the activity of an enzyme for a particular substrate. The catalytic efficiency for the AP-catalyzed hydrolysis of **3** to **4** was, therefore, $k_{cat}/K_M = (1.0 \pm 0.1) \times 10^4$ M^{-1} s^{-1}.

Martinez *et al.* reported that the catalytic efficiency of AP (derived from *Escherichia coli*) for the hydrolysis of a particularly reactive substrate, *p*-nitrophenyl phosphate, was $k_{cat}/K_M = 2.1 \times 10^6$ M^{-1} s^{-1}.[76] From the analysis reported here, we conclude that the k_{cat}/K_M value for the AP-catalyzed hydrolysis of **3** by an AP enzyme derived from bovine intestinal mucosa was a factor of ~200 times lower than the values reported or estimated from established techniques for the hydrolysis of *p*-nitrophenyl phosphate by an AP enzyme derived from *E. coli*.[76] Since the catalytic efficiency is the ratio of k_{cat} and K_M, we evaluated factors that may contribute to the discrepancy between the values of these two parameters with literature values individually.

In order to provide a comparison between the k_{cat} value obtained from the ion channel experiments performed here with the k_{cat} value obtained from an independent technique, we measured the observed rate constant (k_{cat}) of the AP-catalyzed hydrolysis of **5** (Figure 2) by ^{1}H NMR[77] and obtained a value of $k_{cat} = 4.4$ s^{-1}.[78] This value for k_{cat} of the AP-catalyzed hydrolysis of substrate **5** does not, however, provide the best estimate for the k_{cat} value of substrate **3** because the chemical nature of substrates **3** and **5** is very different.[77,79,80] Han and Coleman reported that structural differences in substrates can result in variations in k_{cat} by a factor of 2.5×10^3 for AP-catalyzed hydrolyses of monophosphates.[77] In particular, the k_{cat} values of AP depend strongly on the pK_a values of the hydroxyl group that is cleaved from phosphate monoesters.[77] For instance, the pK_a of dodecanol, which contains a large hydrophobic tail, is 16.2, whereas the pK_a value of methanol is 15.5; this difference in pK_a values translates to a 13-fold lower k_{cat} value of AP-catalyzed hydrolysis of dodecyl phosphate compared to methyl phosphate.[77] For the specific comparison made here, we expect the k_{cat} values for the hydrolysis of **3** to be significantly lower than for the hydrolysis of **5** because the hydrolysis product of **3** contains a large hydrophobic moiety (gA) whereas the hydrolysis product of **5** (ethylenediamine-*N*-glycolate) is a small hydrophilic molecule.[81]

The reported K_M values for monophosphate substrates of AP (from a variety of different organisms and tissue origins) fall in the range of 15 μM to 3 mM.[76,79] The value for $K_M = 0.30 \pm 0.04$ μM obtained here for the AP-catalyzed hydrolysis of **3** to **4** is a factor of 50 below this range. At least four possible reasons could account for the discrepancy between the values of K_M obtained from single ion channel measurements compared to the estimated values obtained by other methods.[76,79] First, the presence of the gramicidin peptide on substrate **3** could enhance the binding affinity of AP to **3**. Second, the presence of a membrane during the enzymatic reaction may affect the value of K_M. The agreement between the values of initial velocities from *in situ* and *ex situ* experiments, however, suggests that the K_M values for **3** were similar under these two different experimental conditions. Third, estimation of K_M values for AP depend on pH but are often reported from measurements at different pH values.[79] A possible fourth reason for the observed discrepancy is that estimates of K_M are most accurate when measurements are performed at concentrations of enzyme that are near the K_M of the enzyme−substrate complex.[72,73] The highest concentration of enzyme that we could use to monitor the AP-catalyzed hydrolysis of **3** to **4** *via* single ion channel conductance measurements (here, 0.6 μM) was at least 25-fold lower than the lowest reported K_M value.[76] The reason why we could not use concentrations of AP higher than 0.6 μM is the extreme sensitivity of the ion channel assay. Given the extremely low concentration of enzyme (here, in the range from 60 pM to 600 nM) that can be monitored by this method, an ion channel-based assay is particularly attractive for analyzing the kinetics of an enzyme if the K_M value for a given substrate is in the picomolar to nanomolar range. This capability is not typically attainable with existing techniques.

The opportunity to quantify enzyme-catalyzed conversions of substrates attached to an ion pore is an attractive and unique characteristic of sensors that are based on ion channel-forming peptides that partition

in and out of the lipid membrane. This reversible partitioning makes it possible to estimate the ratio of gA substrates and gA products during the reaction; that is, the measured ratio between the number of single channel events from products to single channel events from substrate reflects the canonical distribution of $\sim 10^8$ gA molecules in each bilayer chamber. The shift of this distribution over time then yields kinetic information for the enzyme-catalyzed reaction. Gramicidin A is a peptide with such reversible partitioning properties in a membrane. In contrast, covalently attaching a substrate to α-hemolysin, the most commonly used protein pore for nanopore sensing,[43] would not be a suitable strategy for determining enzyme kinetics since α-hemolysin pores typically remain in the bilayer upon integration and do not partition between the membrane and the electrolyte buffer. Consequently, the response of hemolysin-based sensors is stochastic and, unless parallel recordings can be performed in large numbers or a large number of open pores could be monitored in the same bilayer with high precision, alternative design strategies (such as translocation of the enzyme cleavage products through permanently incorporated pores[27−29]) would be necessary to yield suitable statistics for kinetic information.

A gA-Based Sensor for Detection of Anthrax Lethal Factor. In order to test if this ion channel-based assay could be adapted to a second class of enzymes, we explored the possibility of detecting the proteolytic activity of anthrax lethal factor (LF). We chose this particular protease due to its relevance in the context of bioterrorism.[82] In order to adapt the ion channel-based assay platform to LF, we designed a gA derivative that carried a covalently attached peptide substrate for LF.[83−85] Figure 2 shows the amino acid sequence of this gA−LF substrate (**6**). We hypothesized that LF-catalyzed, proteolytic removal of four positive charges from this gA derivative (**6**) would yield a product with significantly increased single-channel conductance since the resulting product contained only one instead of four positive charges close to the entrance of the gA pore. We,[30,38,53] and others,[68,86] demonstrated in previous work that positive charges near the entrance of a gA pore reduce the single channel conductance of these pores due to electrostatic repulsion of the monovalent cations that are transported through gA pores. This effect is particularly pronounced in electrolyte solutions with low ionic strength[30] as used in the work presented here.

Figure 7 demonstrates that the addition of 10 nM LF to a bilayer chamber containing 250 pM gA−LF substrate **6** indeed caused a dramatic increase in the flux of ions through the planar lipid bilayer. Control experiments, in which we added the same concentration of denatured LF or of another enzyme, AP, showed no increase in current (Figure 7B). Interestingly, as shown in Figure 7B, the gA−LF substrate **6** did not generate any significant ion channel activity before addition of active

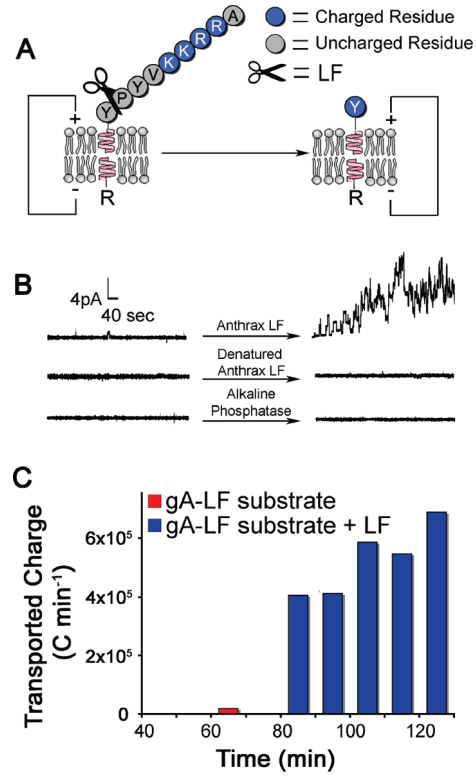

Figure 7. Detection of the functional activity of anthrax lethal factor (LF) based on ion channel amplification. (A) Cartoon illustrating the cleavage of a gA−LF substrate 6 by LF, resulting in the removal eight amino acids (comprising four positive charges) near the opening of a gA pore. The resulting gA product carries one positive charge at the amino terminus of tyrosine (Y). (B) Original current *versus* time traces demonstrating the large increase in transmembrane current after addition of 10 nM LF to a bilayer setup containing 250 pM gA−LF substrate 6; this large increase in transmembrane current is not observed upon addition of denatured LF or another enzyme (here, AP) to the bilayer setup containing gA−LF substrate 6. (C) Time-dependent increase of the flux of electric charge transported across the bilayer (Q, C min^{-1}) as a function of the time after addition of 10 nM LF (which was added here at time = 70 min) to a bilayer containing 250 pM gA−LF substrate 6 in a recording buffer containing 100 mM CsCl, 1 mM HEPES, pH 7.

LF. As discussed previously, we expected that this gA−LF substrate **6** would generate ion channel activity but with significantly reduced single channel conductance compared to native gA. To our surprise, the design of this substrate even exceeded our expectations in the sense that it caused a dramatic response to LF activity from no detectable ion channel activity to a rapidly increasing activity, as illustrated in Figure 7B,C. We propose two possible mechanisms for this attractive characteristic of the gA−LF substrate: (1) The presence of four positive charges on the gA−LF substrate rendered this peptide sufficiently water-soluble such that the resulting low concentration of gA in the lipid membrane made the formation of dimeric gA pores very rare.[87] Removal of four charges from **6** by LF, leading to only one positive charge on the gA product, may shift the partition coefficient of the gA derivative sufficiently to result in frequent formation of

pores.[30,77,88] (2) The presence of nine additional amino acids at the entrance of the gA pore may block the pore sterically, thereby hindering monovalent cations in solution from entering the pore. The presence of four positive charges on these nine amino acids in **6** may have contributed to this blocking effect due to electrostatic attraction of these positively charged amino acid residues to the mouth of the pore (since gA preferentially conducts positively charged ions from solution through its pore).[68] Removal of eight amino acids by LF, leading to a gA derivative with only one additional amino acid compared to native gA, may then have resulted in open gA pores and explain the increase in single ion channel activity upon addition of LF. In this discussion, we excluded a third mechanism that may seem plausible as well, namely, that the presence of four positive charges close to the entrance of the pore in **6** led to electrostatic repulsion of monovalent cations near the opening of the pore, causing a reduction of the single channel conductance through **6** below the detection limit. In this case, we would have expected that elevating the concentration of **6** would lead to an increase of unresolved channel openings with very low single channel conductance that would appear as a gradual increase in the recorded transmembrane current. We did not observe such a gradual increase in current upon addition of increasing concentrations of **6** (up to 0.25 nM) and, hence, concluded that this mechanism is not responsible for the observed on/off signal for detection of LF.

The strong response upon addition of LF to substrate **6** shows that the principle of exploiting ion channel amplification to sense enzyme activity is not limited to sensing based on modulating the local concentration of charge carriers close to the membrane; instead, alternative mechanisms such as removing or introducing steric blockage[68] or modulating the amphiphilic character of chemically modified ion channel-forming peptides provide additional strategies for sensing enzymatic reactions. In particular, the mechanism that involves modulating the amphiphilic character of the pore-forming agent is attractive because it makes it possible to exploit a third amplification effect in addition to enzymatic amplification and ion channel amplification; namely, amplification due to increased (or decreased) partitioning of the pore-forming peptide product into the bilayer compared to substrate. This work, therefore, introduces the idea of a sensor based on inactive pro-channels, which, upon reaction with enzymes, partition strongly into the membrane and form readily detectable ion pores.

In conclusion, this work demonstrates that an ion channel platform based on gA can be employed to detect and monitor the activity of two different enzymes in solution. This detection modality takes advantage of two-fold amplification (the catalytic turnover properties of enzymes and the amplification characteristics of ion flux through a single ion channel pore) to detect enzyme activity with high sensitivity. The ability to follow the conversion of substrate to product over time in the presence of different concentrations of enzymes made it possible to estimate the observed rate constant (k_{cat}), the Michaelis constant (K_M), and the catalytic efficiency of the enzyme using only picomolar concentrations of substrate and picomolar to nanomolar concentrations of enzyme. Although the results described here demonstrate that ion channels can be employed to detect femtomoles to picomoles of the enzymes alkaline phosphatase and anthrax lethal factor using a conventional bilayer setup, increasingly available automated, microfabricated,[41,89−95] and chip-based[39−42] bilayer platforms can improve the stability of membranes as well as reduce the volume of electrolyte solutions required for single ion channel measurements. Implementing such technological advances may make it possible to increase the robustness of these membrane-based sensors as well as to push the detection limit of ion channel platforms to subfemtomole quantities of active enzymes in solution. These novel, automated techniques may also render ion channel recordings accessible for a broad community by overcoming the requirement for specialized expertise.[91,96] In addition, recent advances in chemical synthesis may make it possible to extend this ion channel-based approach to detection of a wide range of enzymes (such as disease-specific phosphatases[97] and kinases[98]).[52,57−63] Due to its nanoscale size and single molecule detection characteristics, an ion channel-based sensing strategy is particularly attractive for detecting enzyme activity within small volumes (such as, potentially, detecting enzyme activity within individual cells by using patch clamp recordings).

METHODS

We purchased all reagents and chemicals from Sigma-Aldrich unless otherwise stated. Gramicidin A (gA) was purchased as gramicidin D from Sigma-Aldrich and purified to a final purity of 97% of gA by silica chromatography using a literature procedure.[99] Alkaline phosphatase from bovine intestinal mucosa (AP, EC 3.1.3.1) and glycolic acid were from Sigma-Aldrich, Inc. Anthrax lethal factor (LF) from recombinant *Bacillus anthracis* (lot# 1722B10A) was purchased from List Biological Laboratories, Inc. The peptide substrate for LF (Ac-AR(Pbf)R(Pbf)K(Boc)K(Boc)VYPY-OH) was purchased from Biopeptide Co., Inc. (purity 98%). We purchased 1,2-diphytanoyl-*sn*-glycero-3-phosphocholine (DiPhyPC) lipids from Avanti Polar Lipids, Inc. All analyses by HPLC were performed on an Agilent Zorbax C-18 column (4.6 μm × 25 cm) using a gradient of 60−100% MeOH in H_2O and a flow rate of 1 mL min^{-1} over 52 min unless otherwise stated.

Synthesis of Benzyl Glycolate.[100] Glycolic acid (200 mg, 2.6 mmol) and triethylamine (401 μL, 2.86 mmol) were dissolved in 2.6 mL of acetone. After 2 min of stirring, benzyl bromideAfter 2 min of stirring, benzyl bromide (279 μL, 2.34 mmol) was added to the

solution. The reaction was refluxed at 60 °C for 12 h. The solution was filtered to remove precipitated triethylammonium bromide and concentrated *in vacuo*. Purification was done by silica chromatography using dichloromethane (DCM) as eluent to remove the nonpolar impurities, and then the eluent was switched to 2% ethyl acetate (EtOAc) in DCM to elute the desired product as a colorless oil (200 mg, 51% yield): ^{1}H NMR (400 MHz, $CDCl_3$) δ 7.362 (5H, s), 5.198 (2H, s), 4.201 (2H, s), 3.366 (1H, s) ppm.

Synthesis of Glycolic Acid-*O*-(di-*tert*-butyl) Phosphate.[101] Di-*tert*-butyl-*N*,*N*-diethyl phosphoramidite (0.62 mL, 2.5 mmol), benzyl glycolate (265 mg, 1.6 mmol), and tetrazole (560 mg, 8 mmol) were dissolved in 46 mL of anhydrous tetrahydrofuran (THF). The reaction was stirred at 23 °C for 2 h and then cooled to −78 °C. *m*-Chloro perbenzoic acid (825 mg, 4.8 mmol) was added to the cooled solution and allowed to stir for 20 min at −78 °C followed by warming to 23 °C for 10 min. The solution was concentrated *in vacuo*, and the crude material was dissolved in 30 mL of DCM and washed twice with 40 mL of saturated $NaHCO_3$, dried over Na_2SO_4, and concentrated *in vacuo*. The resulting crude oil was purified by preparative silica chromatography using DCM/acetone (9:1) to afford 240 mg of yellow oil. The compound was dissolved in 1.5 mL of methanol (MeOH) and subjected to 1 atm hydrogen over 240 mg Pd/C for 3 h. After filtration over Celite, the filtrate was concentrated *in vacuo* to yield a pure colorless liquid (180 mg, 40% yield): ^{1}H NMR (300 MHz, CD_3OD) δ 4.477 (2H, d, J = 9 Hz), 1.408 (18H, s); ^{31}P NMR (300 MHz, CD_3OD) δ −10.437 ppm using an internal ^{31}P NMR standard of 85% phosphoric acid.

Synthesis of Glycolic Acid-*O*-Phosphate, 1.[102] Glycolic acid-*O*-(di-*tert*-butyl) phosphate (6 mg, 22 μmol) was added to a 1.5 mL solution of 1:1 DCM/trifluoroacetic acid (TFA), and the resulting mixture was stirred at 23 °C for 3 h. The resulting solution was concentrated to dryness to yield a clear film of product (3.1 mg, 91% yield): ^{1}H NMR (300 MHz, CD_3OD) δ 4.477 (2H, d, J = 9 Hz); ^{31}P NMR (300 MHz, CD_3OD) δ 3.33 ppm using an internal ^{31}P NMR standard for 85% phosphoric acid.

Synthesis of *O*-Trityl Glycolic Acid.[103] A solution of glycolic acid (800 mg, 10.5 mmol) and of diisopropylethylamine (DIEA, 2.75 g, 9.9 mmol) was prepared in 5 mL of DCM. The resulting mixture was cooled to 0 °C. A solution of trityl chloride (1.62 g, 37.6 mmol) in DCM was added dropwise to this cooled solution. The reaction was stirred for 1 h at 0 °C and then 18 h at 23 °C. The solution was concentrated *in vacuo*. The reaction mixture was purified by silica chromatography using DCM as the eluent until all of the unreacted trityl chloride eluted. The polarity of eluent was increased to 45:4 (DCM/MeOH) to elute *O*-trityl glycolic acid. Upon concentration *in vacuo*, a white solid (902 mg, 22% yield) of *O*-trityl glycolic acid was obtained: ^{1}H NMR (400 MHz, $CDCl_3$) δ 3.89 (2H, s), 7.27−7.36 (9H, m), 7.47 (6H, d, 8 Hz).

Synthesis of Desethanolamine gA. Gramicidin A (142 mg, 75 μmol) was added to 10 mL of acetonitrile (ACN). Phosphorus oxychloride (287 μL, 3 mmol) was added dropwise to the solution of gA, and the reaction was stirred at 23 °C for 4 h. The reaction mixture was concentrated to dryness, and 10 mL of a 4:1 mixture of ACN/H_2O was added. The mixture was stirred for 20 min, concentrated to dryness, and dissolved in 5 mL of a 2:1 mixture of DCM/MeOH. This mixture was added dropwise to a stirred beaker containing 200 mL of H_2O. The resulting precipitate of 2-aminoethyl gramicidate was collected by filtration. The crude yield was 96% by weight. The retention time by HPLC was 34.7 min: ESI-MS (*m*/*z*) calculated for $C_{99}H_{140}N_{20}O_{17}$ (M^+) 1882.07, found $(M - H)^-$ 1880.85.

Anhydrous formic acid (0.55 mL, 14.4 mmol) was combined with acetic anhydride (1.36 mL, 14.4 mmol) and heated to 65 °C for 30 min. After cooling the formic acid/acetic anhydride solution to 23 °C, the mixture was added to 2-aminoethyl gramicidate (139 mg, 72 μmol) that was dissolved in 20 mL of dry THF. The reaction was stirred for 3.5 h followed by concentration to dryness. We dissolved the crude product in a minimal volume of a 2:1 mixture of DCM/MeOH at 23 °C (until the solution was clear) and added this solution dropwise to a stirred beaker containing 200 mL of H_2O. The resulting precipitate of *N*-formyl-2-aminoethyl gramicidate was collected by filtration. The product was isolated by silica chromatography using DCM/MeOH (9:1) as the eluent to afford *N*-formyl-2-aminoethyl gramicidate as a white powder in 72% isolated yield: ESI-MS (*m*/*z*) calculated for $C_{100}H_{140}N_{20}O_{18}$ (M^+) 1910.07, found $(M + Na)^+$ 1932.97.

N-Formyl-2-aminoethyl gramicidate (150 mg, 78 μmol) was dissolved in 25 mL of THF. In a separate flask, $LiOH \cdot H_2O$ (327 mg, 7.8 mmol) was dissolved in 25 mL of H_2O. The two mixtures were combined and stirred at 23 °C for 3 h, followed by slow addition of 1 M HCl until the solution had a pH of 2. The reaction mixture was concentrated *in vacuo* to dryness and redissolved in 15 mL of 2:1 DCM/MeOH. The mixture was added dropwise to 150 mL of H_2O while stirring. The resulting precipitate was collected by filtration and purified by silica chromatography. The eluent initially consisted of a mixture of $CHCl_3$/MeOH/H_2O/acetic acid (750:75:10:2.5) to elute the less polar impurities. After confirming by thin layer chromatography (TLC) that the impurities had eluted, the eluent was changed to $CHCl_3$/MeOH/H_2O/acetic acid (200:30:4:1). The fractions containing desethanolamine gA were concentrated *in vacuo*, and the resulting gel was redissolved in 15 mL of 2:1 DCM/MeOH. The mixture was added dropwise to 150 mL of H_2O while stirring. The resulting precipitate was collected by filtration to yield 93 mg of desethanolamine gA (65% yield over two steps from 2-aminoethyl gramicidate): ESI-MS (*m*/*z*) calculated for $C_{97}H_{135}N_{19}O_{17}$ $(M)^+$ 1839.03, found $(M + Na)^+$ 1861.94. The retention time by HPLC was 40.7 min.

Synthesis of Gramicidamine.[30,52] Desethanolamine gA (25 mg, 13.6 μmol) and triethylamine (7.6 μL, 54.4 μmol) were added to 1 mL of anhydrous THF, and the resulting mixture was stirred and cooled to 0 °C. After adding ethyl chloroformate (5.20 μL, 54.4 μmol) to the cooled mixture, the reaction was stirred for 3.5 h at 0 °C. Mono-*tert*-butyloxycarbonyl (BOC) ethylenediamine (8.6 μL, 54.4 μmol, purchased from Alfa Aesar) was dissolved in 0.2 mL of THF and cooled to 0 °C. This solution was added to the mixture containing desethanolamine gA, and the resulting solution was stirred for an additional 30 min at 0 °C, followed by stirring at 23 °C for 8 h. After concentrating to dryness, the BOC-protected gramicidamine was purified using preparative silica chromatography (using a 9:1 mixture of DCM/MeOH as eluent): ESI-MS (*m*/*z*) calculated for $C_{104}H_{149}N_{21}O_{18}$ (M^+) 1981.14, found $(M - H)^-$ 1979.66. A mixture containing 1 mL of DCM, 1 mL of TFA, 0.1 mL of dimethylsulfide (DMS), and 0.05 mL of ethanedithiol (EDT) was prepared and cooled to 0 °C. BOC-protected gramicidamine (22.4 mg, 11.3 μmol) was dissolved in the cooled mixture. The reaction was allowed to warm up to 23 °C and stirred for 3 h. The reaction mixture was concentrated *in vacuo* to dryness and purified by silica chromatography. The eluent initially consisted of a mixture of DCM/MeOH (9:1) to elute the less polar impurities. After confirming by thin layer chromatography (TLC) that the impurities had eluted, the eluent was changed to DCM/MeOH (9:2): HR-MS (*m*/*z*) calculated for $C_{99}H_{141}N_{21}O_{16}$ $(M + H)^+$ 1881.0937, found $(M + H)^+$ 1881.0943. The retention time by HPLC was 40.5 min. The overall yield was 74% (19 mg) from desethanolamine gA.

Synthesis of gA−Phosphate, 3. *O*-(Di-*tert*-butylphosphate) glycolic acid (3.4 mg, 12.6 μmol) and gramicidamine (8 mg, 4.2 μmol) were dissolved in 2 mL of DCM. Triethylamine (0.72 μL, 15.1 μmol) was added to the solution. After 5 min, 2-ethoxy-1-ethoxycarbonyl-1,2-dihydroquinoline (EEDQ) (3.1 mg, 1.6 μmol) was added and the mixture was stirred for 16 h at 23 °C. The solution was concentrated, and the resulting product was purified using preparative silica chromatography using as eluent a mixture of DCM/MeOH (9:1) to afford 6 mg of a yellow powder. A mixture of 1 mL of 1:1 DCM/TFA, 0.1 mL dimethylsulfide, and 0.02 mL if ethanedithiol was prepared and cooled to 0 °C. The yellow powder was dissolved in this cooled mixture. The reaction was allowed to warm up to 23 °C and stirred for an additional 3 h. The reaction mixture was concentrated and dissolved in 2 mL of 2:1 DCM/MeOH. The mixture was added dropwise to a beaker of 100 mL of water while stirring. The resulting precipitate was collected by filtration as a yellow solid (5.6 mg, 58% yield). For conductance measurements, compound **3** was further purified by RP-HPLC using a Zorbax C-18 column (4.6 × 250 mm), 60% to 92% MeOH in water over 45 min. The retention time was 36.15 min: MALDI-TOF MS (*m*/*z*) calculated for $C_{101}H_{144}N_{21}O_{21}P$ $(M)^+$ 2018.06, found $(M - H)^-$ 2017.21.

Synthesis of 4. Gramicidamine (8 mg, 4.3 μmol) was dissolved in 1.5 mL of THF, and DIEA (3.8 μL, 9.9 μmol) was added. *O*-Trityl glycolic acid (1.7 mg, 8.6 μmol) and EEDQ (2.1 mg, 8.6 μmol) were separately added to the solution. The reaction was stirred for 12 h. The trityl-protected derivative of gramicidamine was purified by preparative silica chromatography with DCM/MeOH (9:1) and was dissolved in 1 mL of DCM and cooled to 0 °C. A solution of 1 mL of TFA/DCM (1:1) with 0.02 mL of dimethylsulfide and 0.01 mL of ethanedithiol was cooled to 0 °C. The TFA solution was then added to the solution containing the trityl-protected derivative of gramicidamine. The reaction was stirred at 23 °C for 4 h. Upon purification by silica chromatography with DCM/MeOH (9:1) as eluent, 6 mg (72% yield) of **4** was obtained: ESI-MS (*m/z*) calculated for $C_{101}H_{143}N_{21}O_{18}$ $(M)^+$ 1939.35, found $(M + Na)^+$ 1962.01.

Synthesis of Ethylenediamine-*N*-glycolate-*O*-phosphate 5. Glycolic acid-*O*-(di-*tert*-butyl) phosphate (3 mg, 11 μmol) was dissolved in 2 mL of THF. *N*-BOC-ethylenediamine (2.1 μL, 13 μmol) and 1-ethyl-3-(3-dimethylaminopropyl)carbodiimide hydrochloride (EDC, 2.5 mg, 13 μmol) were added to the solution. The reaction was stirred for 10 h, and the solution was concentrated *in vacuo*. The protected derivative of **5** was purified by preparative silica chromatography using DCM as eluent. The isolated compound was dissolved in 1 mL of TFA/DCM (1:1). The reaction was stirred for 4 h and concentrated *in vacuo* to afford 1.3 mg (36% yield) of **5** as a TFA salt: ^{1}H NMR (500 MHz, D_2O) δ 4.274 (2H, d, $J = 7.7$ Hz), 3.487 (2H, t, $J = 5.4$ Hz), 3.085 (2H, t, $J = 5.4$ Hz).

Synthesis of gA−LF Substrate 6. Gramicidamine (8 mg, 4.3 μmol) was dissolved in 1.5 mL of THF. Triethylamine (0.72 μL, 15.1 μmol) was added to the solution, and this mixture was chilled to 0 °C. To this solution were added dropwise EDC (1.9 mg, 10 μmol) and the protected peptide substrate for anthrax lethal factor (Ac-AR(Pbf)R(Pbf)K(Boc)K(Boc)VYPY-OH) (15 mg, 8 μmol) in 1.5 mL THF. The reaction was allowed to warm to room temperature over 30 min followed by stirring for 16 h. The solution was concentrated, and the resulting product ($R_f = 0.4$) was purified using preparative silica chromatography using as eluent a mixture of DCM/MeOH (9:2). The purified product was dissolved in 1 mL of DCM and cooled to 0 °C. A solution of 1 mL of TFA/DCM (1:1) with 0.02 mL of dimethylsulfide and 0.01 mL of ethanedithiol was cooled to 0 °C. The TFA solution was then added to the solution containing the protected gA−LF substrate in order to deprotect all of the protecting groups. The reaction was stirred at 23 °C for 3.5 h. The reaction mixture was concentrated *in vacuo* to dryness giving 2.3 mg (17% yield over two steps) of **6** as an off white solid: ESI-MS (*m/z*) calculated for $C_{156}H_{231}N_{38}O_{28}$ $(M + H)^+$ 3086.7, found $(M + H)^+$ 3089.91.

Monitoring the Enzymatic Hydrolysis of Glycolic Acid-*O*-Phosphate 1 with Alkaline Phosphatase by ^{31}P NMR. Glycolic acid-*O*-phosphate **1** (1.1 mg, 7.1 μmol) was added to a buffer containing 100 mM KCl and 140 mM Na_2CO_3 buffer in 0.5 mL of D_2O at pD 9.4. Alkaline phosphatase (0.5 mg, 1 nmol) was added to the solution, and ^{31}P NMR spectra were taken at various time points to monitor the enzymatic hydrolysis of glycolic acid-*O*-phosphate **1** to glycolic acid **2**: ^{31}P NMR (300 MHz, D_2O) glycolic acid-*O*-phosphate, δ 3.33 ppm; free inorganic phosphate, 2.54 ppm using an internal 85% phosphoric acid standard (set to 0 ppm). The reaction appeared to reach completion after 50 min.

Monitoring the Enzymatic Hydrolysis of Ethylenediamine-*N*-glycolate-*O*-phosphate 5 with Alkaline Phosphatase by ^{1}H NMR. Compound **5** (0.58 mg, 3 μmol) was added to a buffer containing 100 mM KCl and 140 mM Na_2CO_3 in 0.2 mL of D_2O at pD 9.4. Alkaline phosphatase (0.5 mg, 1 nmol) was added to the solution, and ^{1}H NMR spectra were taken using a single scan at 3 min intervals to monitor the enzymatic hydrolysis of the phosphate **5** to ethylenediamine-*N*-glycolate. No visible saturation of the NMR signal due to insufficient relaxation times was observed under these conditions. The integral of the doublet in **5** was compared to the corresponding singlet in the product. The k_{cat} of this AP-catalyzed hydrolysis was estimated from the formation of product over time in an analogous manner as reported previously.[23] **5**: ^{1}H NMR (500 MHz, D_2O) δ 4.274 (2H, d, $J = 7.7$ Hz), 3.487 (2H, t, $J = 5.4$ Hz), 3.085 (2H, t, $J = 5.4$ Hz). Ethylenediamine-*N*-glycolate: δ 3.891 (2H, s), 3.139 (2H, t, $J = 5.4$ Hz), 2.988 (2H, t, $J = 5.4$ Hz).

Formation of Planar Lipid Bilayers. We formed planar lipid bilayers by the "folding technique" over an aperture with a diameter ~150 μm in a Teflon film as described previously.[30] The recording electrolyte was 1 mM $MgCl_2$, 50 mM CsCl buffered with 0.5 mM K_2CO_3 at pH 9.8. Briefly, we spread a solution containing 25 mg mL^{-1} 1,2-diphytanoyl-*sn*-glycero-3-phosphatidylcholine (DiPhyPC) lipids in pentane at the air−water interface of the electrolyte solution in both compartments of the bilayer setup. We aspirated 3 mL of the total volume of 4 mL of electrolyte solution in each bilayer compartment into a syringe, followed by dispensing the electrolyte solution back into each compartment. We repeated this cycle of raising and lowering the liquid levels until we obtained a bilayer that had a minimum capacitance of 70 pF and that was stable (*i.e.*, no significant current fluctuations above the baseline noise level) at ±100 mV of applied potential for at least 2 min.

Ion Channel Measurements. We performed single channel recordings in "voltage clamp mode" using Ag/AgCl pellet electrodes (Warner Instruments) in both compartments of the bilayer setup. Data acquisition and storage was carried out using custom software in combination with an EPC-7 patch clamp amplifier from Heka (set at a gain of 10 mV pA^{-1} and a filter cutoff frequency of 3 kHz). The data acquisition board (National Instruments, Austin, TX) that was connected to the amplifier was set to a sampling frequency of 15 kHz. The current traces shown in Figure 3 and Figures S1 and S2 in the Supporting Information were further filtered using a digital Gaussian low-pass filter with a cutoff frequency of 4 Hz.

We performed the analysis of the single channel current traces by computing histograms of the currents from the original current *versus* time traces with ClampFit 9.2 software from Axon Instruments. From these histograms, we extracted the main current values by fitting a Gaussian function to the peaks in the histograms. All conductance values were obtained from the slopes of $I-V$ curves.[30]

Procedure for Monitoring the Enzymatic Hydrolysis of 3 in the Presence of AP Using Single Ion Channel Recordings. For *in situ* measurements, we added 1 μL (from a 100 ng mL^{-1} solution in ethanol) of **3** (to afford a final concentration of 15 pM of **3**) to both compartments of a bilayer setup containing recording electrolyte. We also added a solution of AP to both compartments. Ion channel events were recorded (typically under an applied potential of +100 mV) continuously over the course of the reaction. For *ex situ* experiments, we added **3** (to a final concentration of 150 pM) and AP (to a final concentration of 6 pM to 6 nM) to recording buffer that contained 2 μM BSA to stabilize AP at low concentrations. We recorded single ion channel events during a 10 min time window once a day (50−250 events) over the course of 4 days by filling both compartments of the bilayer setup with 4 mL from each of these solutions with the desired AP concentration. We estimated the fraction of ion channel events from **4** in the reaction mixture at each time point by counting the number of observed single ion channel events corresponding to the conductance of **3** and **4** within 5 or 10 min time windows. Before addition of AP, ion channel recordings occasionally showed a percentage of events (typically <5%) that corresponded to impurities of the hydrolysis product **4** in the samples of gA phosphate **3**. In these cases, we represented the data as the fraction of events that we recorded from gA derivative **4** (f_4) with respect to the fraction of events from **4** before addition of AP such that $f_4 = (f_t - f_0)/(1 - f_0)$; f_t = fraction of events from **4** at time t and f_0 = fraction of events from **4** before addition of AP (*i.e.*, all points are shown relative to the background of events from **4** in the absence of AP). The capacitance of the folded membranes throughout the course of these studies ranged from 69 to 81 pF.

Procedure for Monitoring the Enzymatic Cleavage of 6 in the Presence of LF Using Single Ion Channel Recordings. Typically, we added 10 μL (from a 100 ng mL^{-1} solution in ethanol) of **6** to both compartments of a bilayer setup containing recording electrolyte. The current across the planar lipid bilayer was monitored at an applied potential of +100 mV continuously for several hours during which time an extremely small number of channel opening or closing events were observed. Using identical conditions, the experiment was repeated and fresh LF (10 nM) was added 1 h after the addition of **6**. The subsequent increase in frequency of

channel opening events was quantified by integrating the area under current *versus* time trace to give the total charge transported per minute. To verify that the increase in frequency of channel opening was not the result of other factors than the cleavage of the gA−LF substrate, we repeated the experiment but added denatured LF (the enzyme was heat-denatured at 80 °C for excess of 6 h)[104] instead of active enzyme and observed that the frequency of events was similar to that when no LF was added. The capacitance of the folded membranes throughout the course of these studies ranged from 69 to 104 pF.

Acknowledgment. This work was supported by a Hellman Faculty Fellowship for J.Y., the UCSD Center for AIDS Research (NIAID 5 P30 AI36214), a National Science Foundation CAREER Award to J.Y. (CHE-0847530), and a National Science Foundation CAREER Award to M.M. (Grant No. 449088). M.X.M. acknowledges support from a UC TSR&TP graduate research fellowship and a California Space Grant Consortium graduate fellowship. The authors are grateful to Professor Charles Perrin for helpful discussions.

Supporting Information Available: Additional *I*−*V* curves and *I*−*t* traces for **3** and **4**, *I*−*t* traces and histograms from *in situ* experiments for the AP-catalyzed hydrolysis of **3**, and the complete author list of refs 24 and 83. This material is available free of charge *via* the Internet at http://pubs.acs.org.

REFERENCES AND NOTES

1. Katus, H. A.; Remppis, A.; Looser, S.; Hallermeier, K.; Scheffold, T.; Kübler, W. Enzyme Linked Immuno Assay of Cardiac Troponin T for the Detection of Acute Myocardial Infarction in Patients. *J. Mol. Cell. Cardiol.* **1989**, *21*, 1349–1353.
2. Makler, M. T.; Hinrichs, D. J. Measurement of the Lactate Dehydrogenase Activity of Plasmodium Falciparum as an Assessment of Parasitemia. *Am. J. Trop. Med. Hyg.* **1993**, *48*, 205–210.
3. Puleo, P. R.; Meyer, D.; Wathen, C.; Tawa, C. B.; Wheeler, S.; Hamburg, R. J.; Ali, N.; Obermueller, S. D.; Triana, F. J.; Zimmerman, J. L. Use of a Rapid Assay of Subforms of Creatine Kinase MB to Diagnose or Rule Out Acute Myocardial Infarction. *N. Engl. J. Med.* **1994**, *331*, 561–566.
4. Keshaviah, A.; Dellapasqua, S.; Rotmensz, N.; Lindtner, J.; Crivellari, D.; Collins, J.; Colleoni, M.; Thurlimann, B.; Mendiola, C.; Aebi, S. CA15-3 and Alkaline Phosphatase as Predictors for Breast Cancer Recurrence: A Combined Analysis of Seven International Breast Cancer Study Group Trials. *Ann. Oncol.* **2007**, *1*, 1–8.
5. Stolbach, L. L.; Krant, M. J.; Fishman, W. H. Ectopic Production of an Alkaline Phosphatase Isoenzyme in Patients with Cancer. *N. Engl. J. Med.* **1969**, *281*, 757–762.
6. Deren, J. J.; Williams, L. A.; Muench, H.; Chalmers, T.; Zamcheck, N. Comparative Study of Four Methods of Determining Alkaline Phosphatase. *N. Engl. J. Med.* **1964**, *270*, 1277–1283.
7. Garba, I. H.; Gregory, U. AST/ALT Ratio in Acute, Uncomplicated *Falciparum malaria* Infection: Comparison in Relation to the AST/ALT Ratios in Diseases of the Liver. *Int. J. Trop. Med.* **2005**, *2*, 18–40.
8. Bradley, K. A.; Mogridge, J.; Mourez, M.; Collier, R. J.; Young, J. A. T. Identification of the Cellular Receptor for Anthrax Toxin. *Nature* **2001**, *414*, 225–229.
9. Halverson, K. M.; Panchal, R. G.; Nguyen, T. L.; Gussio, R.; Little, S. F.; Misakian, M.; Bavari, S.; Kasianowicz, J. J. Anthrax Biosensor, Protective Antigen Ion Channel Asymmetric Blockade. *J. Biol. Chem.* **2005**, *280*, 34056–34062.
10. Nablo, B. J.; Halverson, K. M.; Robertson, J. W. F.; Nguyen, T. L.; Panchal, R. G.; Gussio, R.; Bavari, S.; Krasilnikov, O. V.; Kasianowicz, J. J. Sizing the *Bacillus anthracis* PA63 Channel with Nonelectrolyte Poly(ethylene glycols). *Biophys. J.* **2008**, *95*, 1157–1164.
11. Pannifer, A. D.; Wong, T. Y.; Schwarzenbacher, R.; Renatus, M.; Petosa, C.; Bienkowska, J.; Lacy, D. B.; Collier, R. J.; Park, S.; Leppla, S. H. Crystal Structure of the Anthrax Lethal Factor. *Nature* **2001**, *414*, 229–233.
12. Petosa, C.; Collier, R. J.; Klimpel, K. R.; Leppla, S. H.; Liddington, R. C. Crystal Structure of the Anthrax Toxin Protective Antigen. *Nature* **1997**, *385*, 833–838.
13. Boyer, A. E.; Quinn, C. P.; Woolfitt, A. R.; Pirkle, J. L.; McWilliams, L. G.; Stamey, K. L.; Bagarozzi, D. A.; Hart, J. C., Jr.; Barr, J. R. Detection and Quantification of Anthrax Lethal Factor in Serum by Mass Spectrometry. *Anal. Chem.* **2007**, *79*, 8463–8470.
14. Laromaine, A.; Koh, L. L.; Murugesan, M.; Ulijn, R. V.; Stevens, M. M. Protease-Triggered Dispersion of Nanoparticle Assemblies. *J. Am. Chem. Soc.* **2007**, *129*, 4156–4157.
15. Sinha, A. K. Colorimetric Assay of Catalase. *Anal. Biochem.* **1972**, *47*, 389–394.
16. Hendricks, C. L.; Ross, J. R.; Pichersky, E.; Noel, J. P.; Zhou, Z. S. An Enzyme-Coupled Colorimetric Assay for S-Adenosylmethionine-Dependent Methyltransferases. *Anal. Biochem.* **2004**, *326*, 100–105.
17. Johannsson, A.; Stanley, C. J.; Self, C. H. A Fast Highly Sensitive Colorimetric Enzyme-Immunoassay System Demonstrating Benefits of Enzyme Amplification in Clinical-Chemistry. *Clin. Chim. Acta* **1985**, *148*, 119–124.
18. Chui, W. K.; Wainer, I. W. Enzyme-Based High-Performance Liquid-Chromatography Supports as Probes of Enzyme-Activity and Inhibition—The Immobilization of Trypsin and Alpha-Chymotrypsin on an Immobilized Artificial Membrane High-Performance Liquid-Chromatography Support. *Anal. Biochem.* **1992**, *201*, 237–245.
19. Samizo, K.; Ishikawa, R.; Nakamura, A.; Kohama, K. A Highly Sensitive Method for Measurement of Myosin ATPase Activity by Reversed-Phase High-Performance Liquid Chromatography. *Anal. Biochem.* **2001**, *293*, 212–215.
20. Rosenberg, D. W.; Roque, H.; Kappas, A. A Fluorometric Method for Measuring Ethoxycoumarin O-Deethylase Activity by Reversed-Phase High-Performance Liquid-Chromatography. *Anal. Biochem.* **1990**, *191*, 354–358.
21. Audebert, P.; Demaille, C.; Sanchez, C. Electrochemical Probing of the Activity of Glucose-Oxidase Embedded Sol−Gel Matrices. *Chem. Mater.* **1993**, *5*, 911–913.
22. Ito, S.; Yamazaki, S.; Kano, K.; Ikeda, T. Highly Sensitive Electrochemical Detection of Alkaline Phosphatase. *Anal. Chim. Acta* **2000**, *424*, 57–63.
23. Ruan, C.; Wang, H.; Li, Y. A Bienzyme Electrochemical Biosensor Coupled with Immunomagnetic Separation for Rapid Detection of *Escherichia coli* O15:H7 in Food Samples. *Trans. ASAE* **2002**, *45*, 249–255.
24. Hocchi, K.; Ohashi, T.; Miura, T.; Sasagawa, K.; Sato, Y.; Nomura, F.; Tomonaga, T.; Sunaga, M.; Kojima, R.; Katayama, K.; *et al.* Development of an ELISA Method for Detecting Immune Complexes between Tissue-Nonspecific Alkaline Phosphatase and Immunoglobulin G. *J. Clin. Lab. Anal.* **2007**, *21*, 322–329.
25. Vega-Warner, A. V.; Gandhi, H.; Smith, D. M.; Ustunol, Z. Polyclonal-Antibody-Based ELISA to Detect Milk Alkaline Phosphatase. *J. Agric. Food Chem.* **2000**, *48*, 2087–2091.
26. In related work, Matile and co-workers reported a fluorimetric method to detect enzyme activity using synthetic pores embedded in large unilamellar vesicles. In this assay, the conversion of a substrate in the presence of enzymes affected the leakage of a dye from the vesicles; see ref 47. In addition, Walker and Bayley showed by assays based on changes in optical density that a pore-forming protein can be activated in the presence of a protease trigger; see: Walker, B.; Bayley, H. A Pore-Forming Protein with a Protease-Activated Trigger. *Protein Eng.* **1994**, *7*, 91–97.
27. Cockroft, S. L.; Chu, J.; Amorin, M.; Ghadiri, M. R. A Single-Molecule Nanopore Device Detects DNA Polymerase Activity with Single-Nucleotide Resolution. *J. Am. Chem. Soc.* **2008**, *130*, 818–820.

28. Clarke, J.; Wu, H. C.; Jayasinghe, L.; Patel, A.; Reid, S.; Bayley, H. Continuous Base Identification for Single-Molecule Nanopore DNA Sequencing. *Nat. Nanotechnol.* **2009**, *4*, 265–270.
29. Zhao, Q.; de Zoysa, R. S. S.; Wang, D.; Jayawardhana, D. A.; Guan, X. Real-Time Monitoring of Peptide Cleavage Using a Nanopore Probe. *J. Am. Chem. Soc.* **2009**, *131*, 6–8.
30. Capone, R.; Blake, S.; Rincon Restrepo, M.; Yang, J.; Mayer, M. Designing Nanosensors Based on Charged Derivatives of Gramicidin A. *J. Am. Chem. Soc.* **2007**, *129*, 9737–9745.
31. Ashkenasy, N.; Sanchez-Quesada, J.; Bayley, H.; Ghadiri, M. R. Recognizing a Single Base in an Individual DNA Strand: A Step toward DNA Sequencing in Nanopores. *Angew. Chem., Int. Ed.* **2005**, *44*, 1401–1404.
32. Gokel, G. W.; Schlesinger, P. H.; Djedovi, N. K.; Ferdani, R.; Harder, E. C.; Hu, J.; Leevy, W. M.; Pajewska, J.; Pajewski, R.; Weber, M. E. Functional, Synthetic Organic Chemical Models of Cellular Ion Channels. *Bioorg. Med. Chem.* **2004**, *12*, 1291–1304.
33. Trauner, D. Potassium Channels: Symmetric, Selective, Sensitive. *Angew. Chem., Int. Ed.* **2003**, *42*, 5671–5675.
34. Banghart, M.; Borges, K.; Isacoff, E.; Trauner, D.; Kramer, R. H. Light-Activated Ion Channels for Remote Control of Neuronal Firing. *Nat. Neurosci.* **2004**, *7*, 1381–1386.
35. Chambers, J. J.; Banghart, M. R.; Trauner, D.; Kramer, R. H. Light-Induced Depolarization of Neurons Using a Modified Shaker K+ Channel and a Molecular Photoswitch. *J. Neurophysiol.* **2006**, *96*, 2792–2796.
36. Banghart, M. R.; Volgraf, M.; Trauner, D. Engineering Light-Gated Ion Channels. *Biochemistry* **2006**, *45*, 15129–15141.
37. Stankovic, C. J.; Heinemann, S. H.; Schreiber, S. L. Photo-Modulated Ion Channels Based on Covalently Linked Gramicidins. *Biochim. Biophys. Acta* **1991**, *1061*, 163–170.
38. Blake, S.; Mayer, T.; Mayer, M.; Yang, J. Monitoring Chemical Reactions by Using Ion-Channel-Forming Peptides. *ChemBioChem* **2006**, *7*, 433–435.
39. Laiwalla, F.; Klemic, K. G.; Sigworth, F. J.; Culurciello, E. An Integrated Patch-Clamp Amplifier in Silicon-on-Sapphire CMOS. *IEEE Trans. Circuits Syst.* **2006**, *53*, 2364–2370.
40. Mayer, M.; Kriebel, J. K.; Tosteson, M. T.; Whitesides, G. M. Microfabricated Teflon Membranes for Low-Noise Recordings of Ion Channels in Planar Lipid Bilayers. *Biophys. J.* **2003**, *85*, 2684–2695.
41. Schmidt, C.; Mayer, M.; Vogel, H. A Chip-Based Biosensor for the Functional Analysis of Single Ion Channels. *Angew. Chem., Int. Ed.* **2000**, *39*, 3137–3140.
42. Sondermann, M.; George, M.; Fertig, N.; Behrends, J. C. High-Resolution Electrophysiology on a Chip: Transient Dynamics of Alamethicin Channel Formation. *Biochim. Biophys. Acta* **2006**, *1758*, 545–551.
43. Gouaux, E. α-Hemolysin from *Staphylococcus aureus*: An Archetype of β-Barrel, Channel-Forming Toxins. *J. Struct. Biol.* **1998**, *121*, 110–122.
44. Hladky, S. B.; Haydon, D. A. Ion Transfer Across Lipid Membranes in the Presence of Gramicidin AI Studies of the Unit Conductance Channel. *Biochim. Biophys. Acta* **1972**, *274*, 294–312.
45. Aidley, D. J.; Stanfield, P. R., *Ion Channels: Molecules in Action*, 1st ed.; Cambridge University Press: Cambridge, UK, 1996; pp 28−31.
46. Stankovic, C. J.; Heinemann, S. H.; Delfino, J. M.; Sigworth, F. J.; Schreiber, S. L. Transmembrane Channels Based on Tartaric Acid−Gramicidin A Hybrids. *Science* **1989**, *244*, 813–817.
47. Das, G.; Talukdar, P.; Matile, S. Fluorometric Detection of Enzyme Activity with Synthetic Supramolecular Pores. *Science* **2002**, *298*, 1600–1602.
48. Hirano, A.; Wakabayashi, M.; Matsuno, Y.; Sugawara, M. A Single-Channel Sensor Based on Gramicidin Controlled by Molecular Recognition at Bilayer Lipid Membranes Containing Receptor. *Biosens. Bioelectron.* **2003**, *18*, 973–983.
49. Mayer, M.; Semetey, V.; Gitlin, I.; Yang, J.; Whitesides, G. M. Using Ion Channel-Forming Peptides to Quantify Protein−Ligand Interactions. *J. Am. Chem. Soc.* **2008**, *130*, 1453–1465.
50. Suarez, E.; De, E.; Molle, G.; Lazaro, R.; Viallefont, P. Synthesis and Characterization of a New Biotinylated Gramicidin. *J. Pept. Sci.* **1998**, *4*, 371–377.
51. Xie, H.; Braha, O.; Gu, L. Q.; Cheley, S.; Bayley, H. Single-Molecule Observation of the Catalytic Subunit of cAMP-Dependent Protein Kinase Binding to an Inhibitor Peptide. *Chem. Biol.* **2005**, *12*, 109–120.
52. Blake, S.; Capone, R.; Mayer, M.; Yang, J. Chemically Reactive Derivatives of Gramicidin A for Developing Ion Channel-Based Nanoprobes. *Bioconjugate Chem.* **2008**, *19*, 1614–1624.
53. Macrae, M. X.; Blake, S.; Mayer, T.; Mayer, M.; Yang, J. Reactive Derivatives of Gramicidin Enable Light- and Ion-Modulated Ion Channels. *Proc. SPIE* **2009**, *7397*, 739709-1–739709-13.
54. Cornell, B. A.; Braach-Maksvytis, V. L.; King, L. G.; Osman, P. D.; Raguse, B.; Wieczorek, L.; Pace, R. J. A Biosensor that Uses Ion-Channel Switches. *Nature* **1997**, *387*, 580–583.
55. Futaki, S.; Zhang, Y.; Kiwada, T.; Nakase, I.; Yagami, T.; Oiki, S.; Sugiura, Y. Gramicidin-Based Channel Systems for the Detection of Protein−Ligand Interaction. *Bioorg. Med. Chem. Lett.* **2004**, *12*, 1343–1350.
56. Determining the kinetics of heterogeneous enzymatic processes is complicated and often not possible. See: Deems, R. A.; Eaton, B. R.; Dennis, E. A. Kinetic Analysis of Phospholipase A2 Activity toward Mixed Micelles and Its Implications for the Study of Lipolytic Enzymes. *J. Biol. Chem.* **1975**, *250*, 9013–9020.
57. Bali, D.; King, L.; Kinm, S. Syntheses of New Gramicidin A Derivatives. *Aust. J. Chem.* **2003**, *56*, 293–300.
58. Borisenko, V.; Zhang, Z.; Woolley, G. A. Gramicidin Derivatives as Membrane-Based pH Sensors. *Biochim. Biophys. Acta* **2002**, *1558*, 26–33.
59. Roeske, R. W.; Hrinyopavlina, T. P.; Pottorf, R. S.; Bridal, T.; Jin, X. Z.; Busath, D. Synthesis and Channel Properties of [Tau-16]Gramicidin-A. *Biochim. Biophys. Acta* **1989**, *982*, 223–227.
60. Fields, G. B.; Fields, C. G.; Petefish, J.; Wart, H. E. V.; Cross, T. A. Solid-Phase Peptide Synthesis and Solid-State NMR Spectroscopy of [Ala3-15N][Val1] Gramicidin A. *Proc. Natl. Acad. Sci. U.S.A.* **1988**, *85*, 1384–1388.
61. Rizzolo, F.; Sabatino, G.; Chelli, M.; Rovero, P.; Papini, A. M. A Convenient Microwave-Enhanced Solid-Phase Synthesis of Difficult Peptide Sequences: Case Study of Gramicidin A and CSF114 (Glc). *Int. J. Pept. Res. Ther.* **2007**, *13*, 203–208.
62. Andersen, O. S.; Koeppe, R. E.; Roux, B. Gramicidin Channels. *IEEE Trans. Nanobiosci.* **2005**, *4*, 10–20.
63. Finkelstein, A.; Andersen, O. S. The Gramicidin A Channel: A Review of Its Permeability Characteristics with Special Reference to the Single-File Aspect of Transport. *J. Membr. Biol.* **1981**, *59*, 155–171.
64. Antonenko, Y. N.; Rokitskaya, T. I.; Kotova, E. A.; Reznik, G. O.; Sano, T.; Cantor, C. R. Effect of Streptavidins with Varying Biotin Binding Affinities on the Properties of Biotinylated Gramicidin Channels. *Biochemistry* **2004**, *43*, 4575–4582.
65. Rokitskaya, T. I.; Kotova, E. A.; Antonenko, Y. N. Cytochrome *c* Decelerates Channel Kinetics of Negatively Charged Gramicidin Due to Electrostatic Interaction. *Biochem. Biophys. Res. Commun.* **2003**, *302*, 865–868.
66. Bard, A. J.; Faulkner, L. R. *Electrochemical Methods: Fundamentals and Applications*; Wiley: New York, 1980.
67. Apell, H. J.; Bamberg, E.; Alpes, H.; Lauger, P. Formation of Ion Channels by a Negatively Charged Analog of Gramicidin-A. *J. Membr. Biol.* **1977**, *31*, 171–188.
68. For an alternative explanation of the effect of charged groups on conductance through modified gA pores, see: Reiss, P.; Al-Momani, L.; Koert, U. A Voltage-Responding Ion Channel Derived by C-Terminal Modification of Gramicidin A. *ChemBioChem* **2008**, *9*, 377–379.

69. Millan, J. L. *Mammalian Alkaline Phosphatases: From Biology to Applications in Medicine and Biotechnology*; Wiley-VCH: Weinheim, Germany, 2006.
70. When we incorporated a mixture of **3** and **4** in a planar lipid bilayer (which presumably formed homodimeric gramicidin channels comprised **3**-**3** and **4**-**4** as well as heterodimeric channels composed of **3**-**4**), we observed ion channel events with only two types of conductance values that were similar to the homodimeric channels of either **3**-**3** or **4**-**4** under applied potentials $\geq|\pm 50$ mV| (Figure S1 in the Supporting Information). This result is consistent with our previous report (see ref 30) that showed that the conductance of ions through heterodimeric gramicidin channels comprising a negatively charged and an uncharged derivative of gA adopts approximately the same conductance as homodimeric gramicidin channels (at potentials of $\geq|\pm 50$ mV|); this conductance depends on the charge of the group at the entrance of the pore. The conductance through these heterodimeric channels does not depend on the charge presented near the exit of the pore. Due to the absence of an intermediate conductance from heterodimeric channels, the conversion of **3** to **4** by AP can be monitored unambiguously.
71. Meier, W.; Nardin, C.; Winterhalter, M. Reconstitution of Membrane Proteins in (Polymerized) ABA-Triblock Copolymer. *Angew. Chem., Int. Ed.* **2000**, *39*, 4599–4602.
72. Voet, D.; Voet, J. G.; Pratt, C. W. *Fundamentals of Biochemistry*. Wiley: New York, 2003.
73. Connors, K. A. *Chemical Kinetics: The Study of Reaction Rates in Solution*; Wiley-VCH: New York, 1990.
74. Segal, I. H. *Enzyme Kinetics*; Wiley-Interscience: New York, 1975.
75. Morrison, J. F. Kinetics of the Reversible Inhibition of Enzyme-Catalysed Reactions by Tight-Binding Inhibitors. *Biochim. Biophys. Acta* **1969**, *185*, 269–286.
76. Martinez, M. B.; Flickinger, M. C.; Nelsestuen, G. L. Accurate Kinetic Modeling of Alkaline Phosphatase in the *Escherichia coli* Periplasm: Implications for Enzyme Properties and Substrate Diffusion. *Biochemistry* **1996**, *35*, 1179–1186.
77. We used an NMR method to measure k_{cat} that was similar to the method reported by Han, R.; Coleman, J. E. Dependence of the Phosphorylation of Alkaline Phosphatase by Phosphate Monoesters on the pK_a of the Leaving Group. *Biochemistry* **1995**, *34*, 4238–4245, except we monitored the formation of product over time using ^{1}H NMR (see Methods for details).
78. Due to the requirement of relatively high (millimolar) concentrations of substrate required for NMR experiments, the K_M of the enzyme−substrate complex could not be measured accurately; see refs 74 and 77.
79. Motzok, I.; Branion, H. D. Studies on Alkaline Phosphatases. 2. Factors Influencing pH Optima and Michaelis Constant. *Biochem. J.* **1959**, *72*, 177–183.
80. Heppel, L. A.; Harkness, D. R.; Hilmoe, R. J. A Study of the Substrate Specificity and Other Properties of the Alkaline Phosphatase of *Escherichia coli*. *J. Biol. Chem.* **1962**, *237*, 841–846.
81. We could not perform NMR analysis of the AP-catalyzed hydrolysis of **3** (instead of **5**) due to the poor solubility of **3** at micromolar concentrations in aqueous solutions and the requirement of high micromolar concentrations of substrate for NMR analysis.
82. Inglesby, T. V.; Henderson, D. A.; Bartlett, J. G.; Ascher, M. S.; Eitzen, E.; Friedlander, A. M.; Hauer, J.; McDade, J.; Osterholm, M. T.; O'Toole, T. Anthrax as a Biological Weapon Medical and Public Health Management. *J. Am. Med. Assoc.* **1999**, *281*, 1735–1745.
83. Forino, M.; *et al.* Efficient Synthetic Inhibitors of Anthrax Lethal Factor. *Proc. Natl. Acad. Sci. U.S.A.* **2005**, *102*, 9499–9504.
84. Turk, B. E.; Wong, T. Y.; Schwarzenbacher, R.; Jarrell, E. T.; Leppla, S. H.; Collier, R. J.; Liddington, R. C.; Cantley, L. C. The Structural Basis for Substrate and Inhibitor Selectivity of the Anthrax Lethal Factor. *Nat. Struct. Mol. Biol.* **2003**, *11*, 60–66.
85. Guichard, A.; Park, J. M.; Cruz-Moreno, B.; Karin, M.; Bier, E. Anthrax Lethal Factor and Edema Factor Act on Conserved Targets in Drosophila. *Proc. Natl. Acad. Sci. U.S.A.* **2006**, *103*, 3244–3249.
86. Woolley, G. A.; Zunic, V.; Karanicolas, J.; Jaikaran, A. S.; Starostin, A. V. Voltage-Dependent Behavior of a "Ball-and-Chain" Gramicidin Channel. *Biophys. J.* **1997**, *73*, 2465–2475.
87. The hypothesis that gA−LF substrate **6** is more water-soluble than other gA derivatives is supported by the observation that a significantly higher concentration of peptide (>250 pM) is necessary to observe single ion channel activity compared to the concentration of peptides (10−100 pM) required for most other gA derivatives. At high concentrations of peptide (1 nM), we observe single ion channel activity from **6**. Analysis of single channel currents through **6** (1 nM) *versus* applied potential resulted in Ohmic behavior (R^2 of a linear fit was 0.97, $N = 6$) over the complete voltage range from −120 to +120 mV. The absence of rectifying behavior indicated that electrostatically driven closure of the channels due movement of the charged residues in **6** into the pore did not occur to a detectable extent over this applied potential range.
88. We have observed previously that gA derivatives carrying one positive charge readily partition into membranes and form ion pores; see ref 30.
89. Fertig, N.; Blick, R. H.; Behrends, J. C. Whole Cell Patch Clamp Recording Performed on a Planar Glass Chip. *Biophys. J.* **2002**, *82*, 3056–3062.
90. Jeon, T. J.; Malmstadt, N.; Schmidt, J. J. Hydrogel-Encapsulated Lipid Membranes. *J. Am. Chem. Soc.* **2006**, *128*, 42–43.
91. Malmstadt, N.; Nash, M. A.; Purnell, R. F.; Schmidt, J. J. Automated Formation of Lipid-Bilayer Membranes in a Microfluidic Device. *Nano Lett.* **2006**, *6*, 1961–1965.
92. Shim, J.; Gu, L. Q. Stochastic Sensing on a Modular Chip Containing a Single Ion Channel. *Anal. Chem.* **2007**, *79*, 2207–2213.
93. Uram, J. D.; Ke, K.; Hunt, A. J.; Mayer, M. Label-Free Affinity Assays by Rapid Detection of Immune Complexes in Submicrometer Pores. *Angew. Chem., Int. Ed.* **2006**, *45*, 2281–2285.
94. Mach, T.; Chimerel, C.; Fritz, J.; Fertig, N.; Winterhalter, M.; Fuetterer, C. Miniaturized Planar Lipid Bilayer: Increased Stability, Low Electric Noise and Fast Fluid Perfusion. *Anal. Bioanal. Chem.* **2008**, *390*, 841–846.
95. Kreir, M.; Farre, C.; Beckler, M.; George, M.; Fertig, N. Rapid Screening of Membrane Protein Activity: Electrophysiological Analysis of OmpF Reconstituted in Proteoliposomes. *Lab Chip* **2008**, *8*, 587–595.
96. Farre, C.; Stoelzle, S.; Haarmann, C.; George, M.; Bruggemann, A.; Fertig, N. Automated Ion Channel Screening: Patch Clamping Made Easy. *Expert Opin. Ther. Targets* **2007**, *11*, 557–565.
97. Boutros, R.; Lobjois, V.; Ducommun, B. CDC25 Phosphatases in Cancer Cells: Key Players? Good Target? *Nat. Rev. Cancer* **2007**, *7*, 495–507.
98. Yu, Q. Y.; Sicinska, E.; Geng, Y.; Ahnstrom, M.; Zagozdzon, A.; Kong, Y. X.; Gardner, H.; Kiyokawa, H.; Harris, L. N.; Stal, O.; Sicinski, P. Requirement for CDK4 Kinase Function in Breast Cancer. *Cancer Cell* **2006**, *9*, 23–32.
99. Stankovic, C. J.; Delfino, J. M.; Schreiber, S. L. Purification of Gramicidin A. *Anal. Biochem.* **1990**, *184*, 100–103.
100. Barrish, J. C.; Lee, H. L.; Mitt, T.; Pizzolato, G.; Baggiolini, E. G.; Uskokovic, M. R. Total Synthesis of Pseudomonic Acid C. *J. Org. Chem.* **1988**, *53*, 4282–4295.
101. Thaisrivongs, S.; Pals, D. T.; DuCharme, D. W.; Turner, S. R.; DeGraaf, G. L.; Lawson, J. A.; Couch, S. J.; Williams, M. V. Renin Inhibitory Peptides. Incorporation of Polar, Hydrophilic End Groups into an Active Renin Inhibitory Peptide Template and Their Evaluation in a Human Renin-

Infused Rat Model and in Conscious Sodium-Depleted Monkeys. *J. Med. Chem.* **1991**, *34*, 633–642.
102. Chen, B.; Zhou, X.; Taghizadeh, K.; Chen, J.; Stubbe, J. A.; Dedon, P. C. GC-MS Methods to Quantify the 2-Deoxypentos-4-ulose and 3-Phosphoglycolate Pathways of 4-Oxidation of 2-Deoxyribose in DNA: Application to DNA Damage Produced by Radiation and Bleomycin. *Chem. Res. Toxicol.* **2007**, *20*, 1701–1708.
103. Rijkers, D. T. S.; Hoppener, J. W. M.; Posthuma, G.; Lips, C. J. M.; Liskamp, R. M. J. Inhibition of Amyloid Fibril Formation of Human Amylin by N-Alkylated Amino Acid and Hydroxy Acid Residue Containing Peptides. *Chem.—Eur. J.* **2002**, *8*, 4285–4291.
104. Gupta, P.; Singh, S.; Tiwari, A.; Bhat, R.; Bhatnagar, R. Effect of pH on Stability of Anthrax Lethal Factor: Correlation between Denaturation and Activity. *Biochem. Biophys. Res. Commun.* **2001**, *284*, 568–573.